

12. J. Kim, C. Cho, and J. Lee, 5.2 GHz notched ultra-wideband antenna using slot-type SRR, *Electron Lett* 42 (2006), 315–316.
13. M. Gil, J. Bonache, J. Garcia-Garcia, and F. Martin, Composite right/left handed (CRLH) transmission lines based on complementary split ring resonators (CSRRs) and applications, In: *Proc metamaterials*, Roma, Italy, 2007, pp. 22–24.
14. S. Eggermont and I. Huynen, Leaky wave radiation phenomena in metamaterial transmission line based on complementary split ring resonators, *Microwave Opt Technol Lett* 53 (2011), 2025–2029.
15. J.B. Pendry, A.J. Holden, D.J. Robbins, and W.J. Stewart, Magnetism from conductors and enhanced nonlinear phenomena, *IEEE Trans Microwave Theory Tech* 47 (1999), 2075–2084.
16. R. Marqués, F. Martín, and M. Sorolla, *Metamaterials with negative parameters: Theory, design and microwave applications*, Wiley-Interscience, Hoboken, NJ, 2008.
17. S. Eggermont, I. Huynen, Substrate edge effects in leaky wave antenna based on complementary split ring resonators, In: *Proc EUCAP 2010*, Barcelona, 2010.
18. M. Gil, J. Bonache, I. Gil, J. Garcia-Garcia, and F. Martin, On the transmission properties of left handed microstrip lines implemented by complementary split rings resonators. *Int Numer Model: Electron Networks Devices Fields* 19 (2006), 87–103.

© 2012 Wiley Periodicals, Inc.

SMALL-SIZE WWAN MONOPOLE SLOT ANTENNA WITH DUAL-BAND BAND-STOP MATCHING CIRCUIT FOR TABLET COMPUTER APPLICATION

Kin-Lu Wong and Pei-Ji Ma

Department of Electrical Engineering, National Sun Yat-Sen University, Kaohsiung 804, Taiwan; Corresponding author: wongkl@ema.ee.nsysu.edu.tw

Received 1 July 2011

ABSTRACT: A monopole slot antenna printed on a small-size FR4 substrate of $40 \times 10 \text{ mm}^2$ to provide two wide operating bands of 824–960 and 1710–2170 MHz for the wireless wide area network operation in the tablet computer is presented. The monopole slot is folded to achieve a compact configuration and is fed by a microstrip feedline loaded with a dual-band band-stop matching circuit on the same FR4 substrate. The band-stop matching circuit can generate two separate parallel resonances at about 1050 and 2250 MHz, which respectively leads to additional resonance occurred nearby the resonant frequencies of the quarter-wavelength slot mode at about 850 MHz and higher-order slot mode at about 1900 MHz, thereby resulting in dual-resonance excitation of the two excited slot modes to respectively cover the GSM850/900 and GSM1800/1900/UMTS operation. The bandwidth-enhancement technique of using a dual-band band-stop matching circuit is reported for the first time in published articles, and its detailed operating principle is described in this study. Performances of the proposed antenna are also discussed. © 2012 Wiley Periodicals, Inc. *Microwave Opt Technol Lett* 54:875–879, 2012; View this article online at wileyonlinelibrary.com. DOI 10.1002/mop.26723

Key words: mobile antennas; internal tablet computer antennas; wireless wide area network antennas; printed slot antennas; band-stop matching circuit

1. INTRODUCTION

Using a band-stop, matching circuit has been shown to be effective in leading to a dual-resonance excitation of the antenna's lower band at about 900 MHz for an internal folded loop antenna to cover the WWAN (wireless wide area network) operation in the mobile handset [1]. The obtained lower-band band-

width is more than twice the bandwidth of the case without using a band-stop matching circuit. Hence, with a small antenna volume of 0.6 cm^3 only, this technique of using a band-stop matching circuit makes it easy for the antenna to achieve a wide lower band to cover the GSM850/900 operation (824–960 MHz). For the antenna's wide upper band, it is formed by two higher-order resonant modes of the loop antenna [1] to cover the GSM1800/1900/UMTS operation (1710–2170 MHz). Also note that, in almost all the handsets, a small board space on the system circuit board is generally reserved for disposing the matching circuits [2–5] for the embedded WWAN antenna. The band-stop matching circuit for the internal handset antenna application can be disposed on a similar small board space that is reserved for accommodating the traditional matching circuits.

In this article, we apply a dual-band band-stop matching circuit to a monopole slot antenna printed on a small FR4 substrate of size $40 \times 10 \text{ mm}^2$ for tablet computer applications. Different from the reported band-stop matching circuit used for lower-band bandwidth enhancement only [1], the dual-band band-stop matching circuit in this study can generate two separate parallel resonances and lead to two dual-resonance excitations of the quarter-wavelength and higher-order resonant modes of the monopole slot antenna to greatly enhance the bandwidths of both the antenna's lower and upper bands. Thus, with a small antenna size and a large ground plane (display ground in the tablet computer in this study) that the antenna is connected to, which generally cannot aid in enhancing the antenna's lower-band bandwidth as the relatively small system ground plane in the handset as an efficient radiator [6–10], the proposed planar monopole slot antenna can cover the penta-band WWAN operation in the 824–960 and 1710–2170 MHz bands. Moreover, note that the dual-band band-stop matching circuit is disposed on the ground portion on the FR4 substrate and requires no board space in the system circuit board of the tablet computer. The latter is different from that in the matching circuits used for the handset [1–5] and should be more attractive for practical tablet computer applications.

Compared to the required antenna sizes of the monopole slot antennas that have been reported for the WWAN operation in the notebook or tablet computer with a large ground plane (for example, the antenna size is $60 \times 12 \text{ mm}^2$ in Ref. 11 and $75 \times 10 \text{ mm}^2$ in Ref. 12), the proposed monopole slot antenna has the smallest antenna size of $40 \times 10 \text{ mm}^2$. Also, only one monopole slot is required (in Refs. 12 and 11, two and three monopole slots are respectively required), which leads to a simpler antenna design for the proposed antenna. Details of the proposed monopole slot antenna with the dual-band band-stop matching circuit are presented in the article.

2. PROPOSED ANTENNA

Figure 1(a) shows the proposed small-size WWAN printed monopole slot antenna with detailed dimensions, and the antenna connected to the top shielding metal wall of the display ground for tablet computer application is shown in Figure 1(b). The antenna is printed on a 0.8-mm thick FR4 substrate of size $40 \times 10 \text{ mm}^2$, relative permittivity 4.4, and loss tangent 0.024. There is only one monopole slot required in the proposed design for achieving penta-band WWAN operation. The monopole slot is embedded in the metal plate printed on one side of the FR4 substrate, on which there is a printed ground plane, and the monopole slot is folded to achieve a compact antenna configuration. The antenna ground is grounded to the shielding metal wall of size $5 \times 150 \text{ mm}^2$ at the top edge of the display ground,

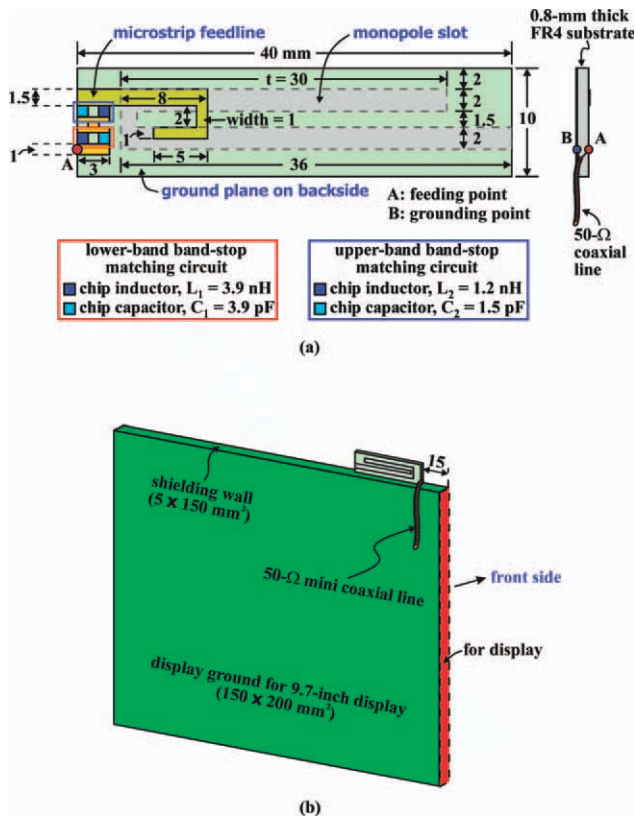


Figure 1 (a) Proposed WWAN printed monopole slot antenna. (b) The antenna connected to the top shielding metal wall of the display ground for tablet computer application. [Color figure can be viewed in the online issue, which is available at wileyonlinelibrary.com]

which has a size of 150×200 mm² to support a 9.7-inch display (not shown in figure). The tablet computer with a 9.7-inch display is very common and commercially available in the market.

The monopole slot has a length of 71.5 mm and can generate its quarter-wavelength resonant mode [13–20] at about 850 MHz and its higher-order resonant mode at about 1900 MHz. However, the obtained bandwidths of the two slot modes are far from covering the desired operating bands. By disposing a dual-band band-stop matching circuit whose equivalent circuit is shown in Figure 2 in the 50-Ω microstrip feedline which feeds the monopole slot, both the bandwidths of the antenna's lower

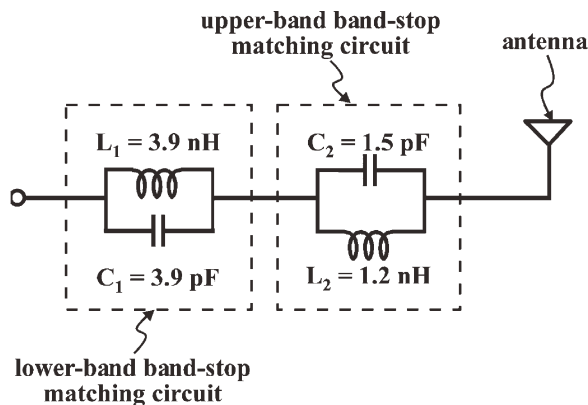


Figure 2 Equivalent circuit of the dual-band band-stop matching circuit for the proposed antenna

and upper bands can be greatly enhanced to cover the desired operating bands. Note that in the proposed folded monopole slot, there are two parallel slot sections respectively with the closed end and the open end. The microstrip feedline is adjusted to extend from the shorter slot section with the closed end to the longer slot section with the open end so that good excitation of the first two resonant modes of the monopole slot can be excited with good impedance matching and occurred at the desired frequency ranges.

The dual-band band-stop matching circuit comprises two single-band band-stop circuits, whose equivalent circuit is shown in Figure 2. The first one (lower-band band-stop circuit) is formed by a 3.9-nH chip inductor and a 3.9-pF chip capacitor connected in parallel and can generate a parallel resonance at about 1050 MHz, which is at the high frequency tail of the quarter-wavelength slot mode and can effectively improve the impedance matching of the same and generate an additional resonance (zero reactance) nearby, thus, resulting in a dual-resonance slot mode to achieve a much wider bandwidth to cover the GSM850/900 operation.

The second (upper-band) band-stop circuit is formed by a 1.2-nH chip inductor and a 1.5-pF chip capacitor connected in parallel. This band-stop circuit can result in a parallel resonance occurred at about 2250 MHz, which is at the high-frequency tail of the higher-order slot mode, and a second additional resonance can be generated at nearby frequencies to result in a dual-resonance excitation of the higher-order slot mode. Hence, a wide upper band is also achieved for the antenna to cover the desired GSM1800/1900/UMTS operation.

Also note that for practical tablet computer applications, a 50-Ω coaxial line is generally used as shown in the figure to connect the antenna to the transceiver (not shown in the figure) disposed on the display ground which serves as the system

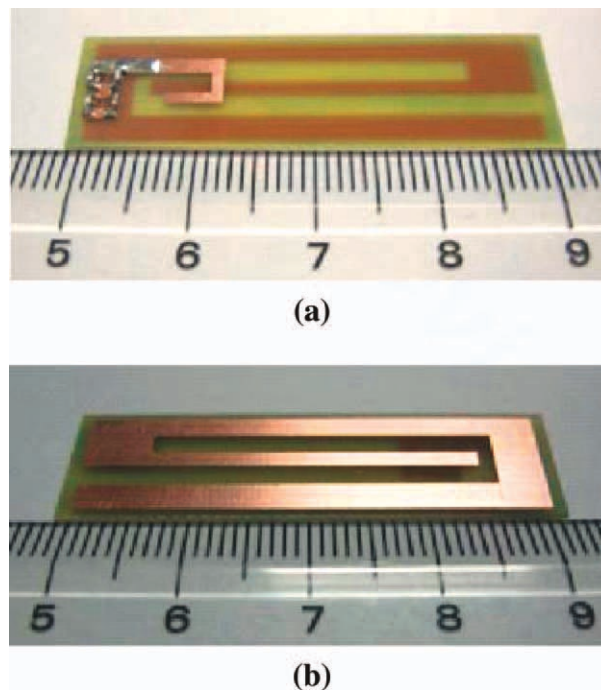


Figure 3 Photos of the fabricated antenna. (a) Viewing from the substrate surface with printed microstrip feedline and band-stop matching circuit. (b) Viewing from the substrate with printed ground plane. [Color figure can be viewed in the online issue, which is available at wileyonlinelibrary.com]

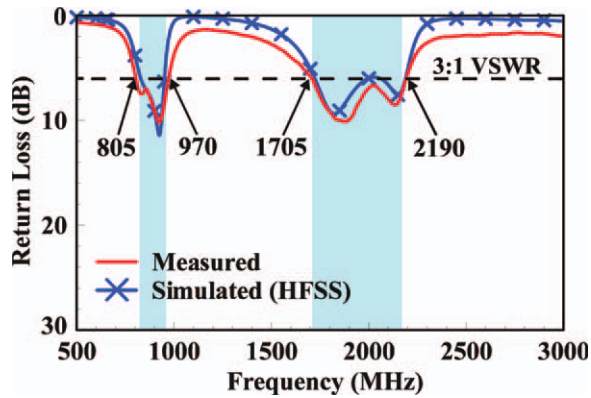


Figure 4 Measured and simulated return loss for the proposed antenna. [Color figure can be viewed in the online issue, which is available at wileyonlinelibrary.com]

ground plane of the tablet computer. In this study for testing the antenna, the central conductor and outer grounding sheath of the coaxial line are respectively connected to point A (feeding point) at the front terminal of the band-stop matching circuit on the front side and point B (grounding point) at the ground plane on the back side. Photos of the fabricated antenna are shown in Figure 3, and the obtained results of the antenna are presented and discussed in Section 3.

3. RESULTS AND DISCUSSION

The fabricated antenna shown in Figure 3 is mounted and connected to the top shielding metal wall of the display ground as shown in Figure 1(b) in the following studies. Results of the measured and simulated return loss for the antenna are shown in Figure 4. Simulated return loss is obtained using full-wave electromagnetic field simulator high frequency structure simulator [21], and agreement between the simulation and measurement is seen. For both the antenna's desired lower and upper bands,

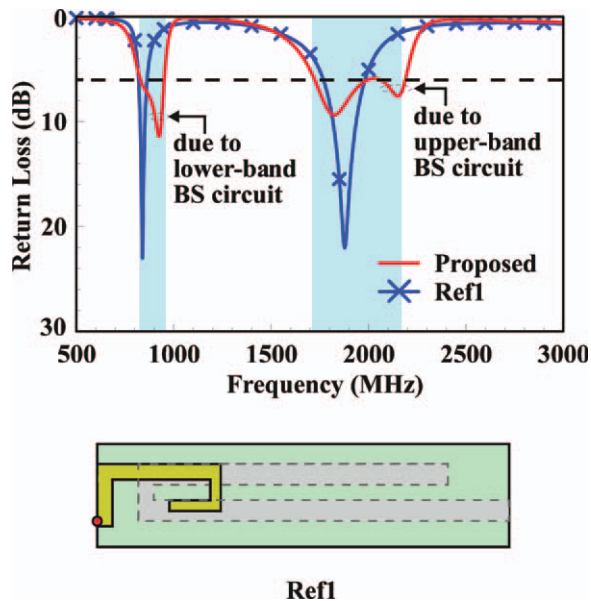


Figure 5 Simulated return loss for the proposed antenna and the case without the dual-band band-stop matching circuit (Ref1). [Color figure can be viewed in the online issue, which is available at wileyonlinelibrary.com]

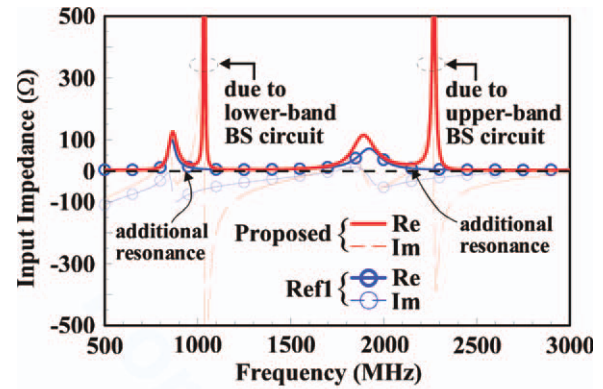


Figure 6 Simulated input impedance of the proposed antenna and Ref1 in Figure 5. [Color figure can be viewed in the online issue, which is available at wileyonlinelibrary.com]

dual-resonance excitation is obtained. The measured return loss for frequencies in the lower and upper bands (the two shaded regions in the figure) are seen to be better than 6 dB (3:1 VSWR), the design specification widely used for the internal WWAN mobile device antennas. That is, the proposed antenna can be applied for practical applications.

To analyze the operating principle of the antenna, Figure 5 shows the simulated return loss for the proposed antenna and the case without the dual-band band-stop matching circuit (Ref1). It is clearly seen that when the dual-band band-stop matching circuit is not present, the excited resonant mode in the lower and upper bands become a single-resonance mode and hence the obtained lower-band and upper-band bandwidths are

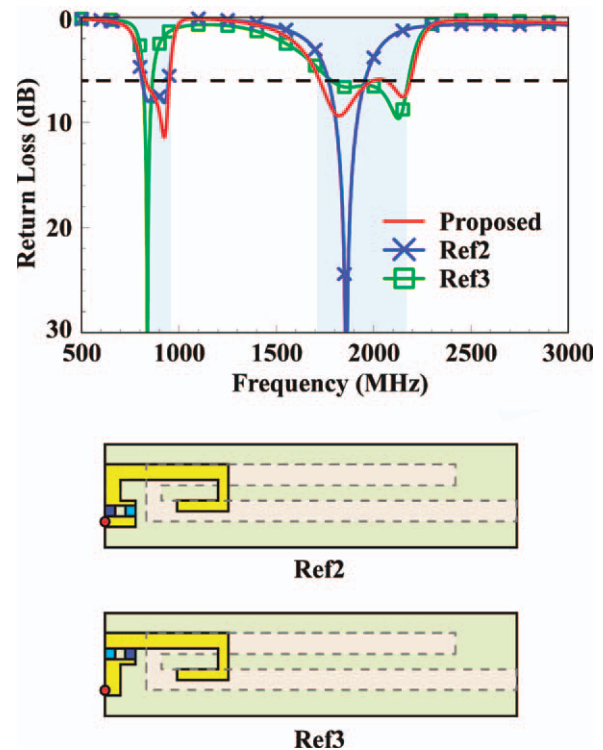


Figure 7 Simulated return loss for the proposed antenna, the case with the lower-band band-stop circuit (Ref2), and the case with the upper-band band-stop circuit (Ref3). [Color figure can be viewed in the online issue, which is available at wileyonlinelibrary.com]

greatly decreased. This behavior can be explained more clearly from the corresponding input impedance of the proposed antenna and Ref1 shown in Figure 6. Because of the dual-band band-stop matching circuit, two parallel resonances are generated at about 1050 and 2250 MHz, which are respectively at the high-frequency tail of the 0.25-wavelength slot mode at 850 MHz and the higher-order slot mode at 1900 MHz. The two parallel resonances lead to additional resonances (zero reactances) at about 900 and 2150 MHz as shown in the figure, which respectively result in dual-resonance lower and upper bands for the proposed antenna. Hence, much larger bandwidths of the antenna's lower and upper bands are achieved.

Figure 7 shows the simulated return loss for the proposed antenna, the case with the lower-band band-stop circuit (Ref2), and the case with the upper-band band-stop circuit (Ref3). For Ref2, only dual-resonance excitation in the lower band is obtained, and the upper band shows a single-resonance excitation. Although for Ref3, only dual-resonance excitation in the upper band is seen, and the lower band shows a single-resonance excitation. The obtained results indicate that the lower and upper bands can generally be controlled by the lower-band and upper-band band-stop matching circuits, respectively.

Figure 8 plots the measured three-dimensional (3D) total-power radiation patterns for the proposed antenna. The radiation patterns are measured in a far-field anechoic chamber, and the full 3D and half 3D (cross-sectional cut in the $y-z$ plane) radiation patterns at five testing frequencies (central frequencies of five WWAN operating bands) are presented. Because of the rel-

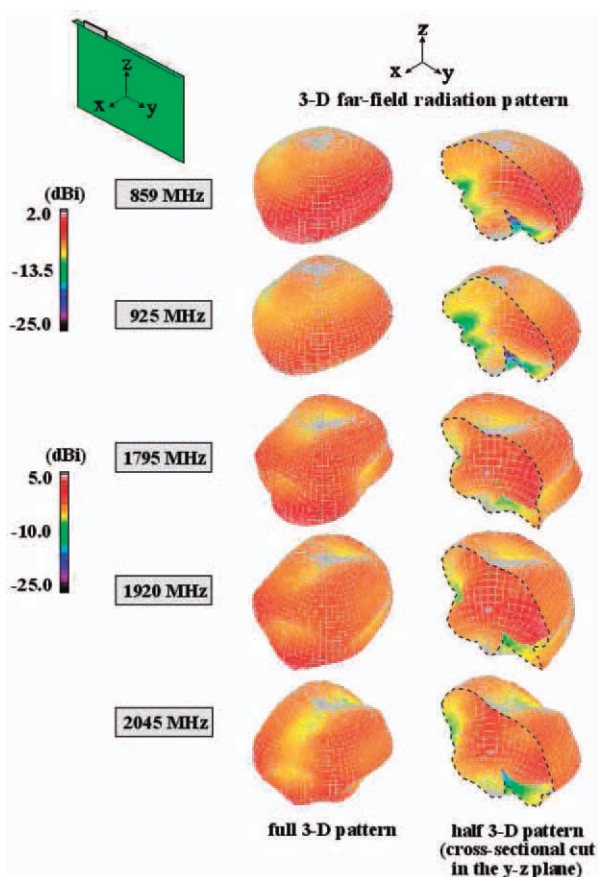


Figure 8 Measured 3D total-power radiation patterns for the proposed antenna. [Color figure can be viewed in the online issue, which is available at wileyonlinelibrary.com]

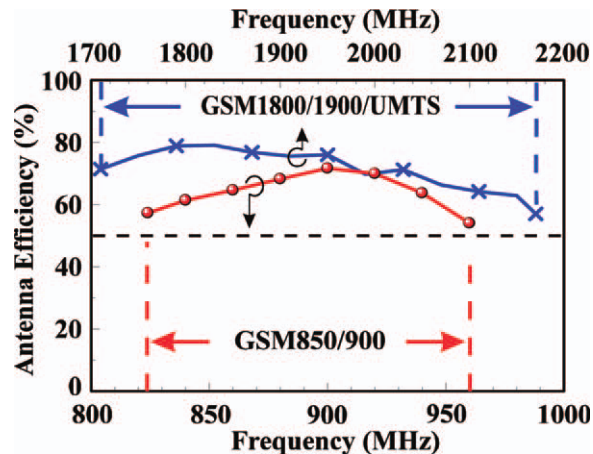


Figure 9 Measured antenna efficiency (mismatching loss included) for the proposed antenna. [Color figure can be viewed in the online issue, which is available at wileyonlinelibrary.com]

atively much larger size of the display ground compared to the system ground plane of the mobile handset or smartphone [22–26], the radiation patterns at lower frequencies of 859 and 925 MHz are no longer close to dipole-like patterns. However, in the azimuthal plane ($x-y$ plane), near-omnidirectional radiation is still observed. At higher frequencies of 1795, 1920, and 2045 MHz, the radiation patterns are different from those at lower frequencies, and there are some dips in the radiation patterns seen in the azimuthal plane. The measured antenna efficiency which includes the mismatching loss for the proposed antenna is shown in Figure 9. Over the desired GSM850/900 and GSM1800/1900/UMTS bands, the measured efficiency is respectively about 53–72 and 57–79%, which are acceptable for practical applications.

4. CONCLUSION

Dual-wideband operation of a small-size planar monopole slot antenna using a dual-band band-stop matching circuit for tablet computer application has been proposed. The proposed design is easy to implement at low cost. The monopole slot antenna with the dual-band band-stop matching circuit is disposed on a small-size FR4 substrate of $40 \times 10 \text{ mm}^2$ only, and two wide operating bands covering the 824–960 and 1710–2170 MHz bands for the penta-band WWAN operation has been obtained. Detailed operating principle of the proposed design has been analyzed in this study. Good radiation characteristics for frequencies over the operating bands have also been obtained. With the obtained results, the proposed antenna is promising for practical tablet computer applications.

REFERENCES

1. Y.W. Chi and K.L. Wong, Very-small-size folded loop antenna with a band-stop matching circuit for WWAN operation in the mobile phone, *Microw Opt Technol Lett* 51 (2009), 808–814.
2. K.L. Wong and T.W. Kang, GSM850/900/1800/1900/UMTS printed monopole antenna for mobile phone application, *Microw Opt Technol Lett* 50 (2008), 3192–3198.
3. M. Tzortzakakis and R.J. Langley, Quad-band internal mobile phone antenna, *IEEE Trans Antennas Propagat* 55 (2007), 2097–2103.
4. Z. Zhang, J.-C. Langer, K. Li, and M.F. Iskander, Design of ultra-wideband mobile phone antenna (824 MHz~6 GHz), *IEEE Trans Antennas Propagat* 56 (2008), 2107–2111.

5. T. Oshiyama, H. Mizuno, and Y. Suzuki, Multi-band antenna, U.S. Patent Publication No. 2007/0249313 A1, October 25, 2007.
6. P. Vainikainen, J. Ollikainen, O. Kivekas, and I. Kellander, Resonator-based analysis of the combination of mobile handset antenna and chassis, *IEEE Trans Antennas Propagat* 50 (2002), 1433–1444.
7. T.Y. Wu and K.L. Wong, On the impedance bandwidth of a planar inverted-F antenna for mobile handsets, *Microw Opt Technol Lett* 32 (2002), 249–251.
8. C.T. Lee and K.L. Wong, Internal WWAN clamshell mobile phone antenna using a current trap for reduced groundplane effects, *IEEE Trans Antennas Propagat* 57 (2009), 3303–3308.
9. W.Y. Li and K.L. Wong, Internal wireless wide area network clamshell mobile phone antenna with reduced ground plane effects, *Microw Opt Technol Lett* 52 (2010), 922–930.
10. Y.W. Chi and K.L. Wong, Compact multiband folded loop chip antenna for small-size mobile phone, *IEEE Trans Antennas Propagat* 56 (2008), 3797–3803.
11. K.L. Wong and L.C. Lee, Multiband printed monopole slot antenna for WWAN operation in the laptop computer, *IEEE Trans Antennas Propagat* 57 (2009), 324–330.
12. K.L. Wong and F.H. Chu, Internal planar WWAN laptop computer antenna using monopole slot elements, *Microw Opt Technol Lett* 51 (2009), 1274–1279.
13. H. Wang, M. Zheng, and S.Q. Zhang, Monopole slot antenna, U.S. Patent No. 6,618,020 B2, September 9, 2003.
14. P. Lindberg, E. Ojefors, and A. Rydberg, Wideband slot antenna for low-profile hand-held terminal applications, In: *Proceedings of 36th European Microwave Conference (EuMC2006)*, Manchester, UK, pp. 1698–1701.
15. K.L. Wong, P.W. Lin, and C.H. Chang, Simple printed monopole slot antenna for penta-band WWAN operation in the mobile handset, *Microw Opt Technol Lett* 53 (2011), 1399–1404.
16. W.S. Chen and K.Y. Ku, Broadband design of a small non-symmetric ground $\lambda/4$ open slot antenna, *Microwave J* 50 (2007), 110–120.
17. C. Hsieh, T. Chiu, and C. Lai, Compact dual-band slot antenna at the corner of the ground plane, *IEEE Trans Antennas Propagat* 56 (2009), 3423–3426.
18. C.I. Lin and K.L. Wong, Printed monopole slot antenna for internal multiband mobile phone antenna, *IEEE Trans Antennas Propagat* 55 (2007), 3690–3697.
19. F.H. Chu and K.L. Wong, Simple folded monopole slot antenna for penta-band clamshell mobile phone application, *IEEE Trans Antennas Propagat* 57 (2009), 3680–3684.
20. C.I. Lin and K.L. Wong, Printed monopole slot antenna for penta-band operation in the folder-type mobile phone, *Microw Opt Technol Lett* 50 (2008), 2237–2241.
21. <http://www.ansys.com/products/hf/hfss/>, ANSYS HFSS, Ansoft Corp, Pittsburgh, PA.
22. K.L. Wong, W.Y. Chen, and T.W. Kang, On-board printed coupled-fed loop antenna in close proximity to the surrounding ground plane for penta-band WWAN mobile phone, *IEEE Trans Antennas Propagat* 59 (2011), 751–757.
23. F.H. Chu and K.L. Wong, Simple planar printed strip monopole with a closely-coupled parasitic shorted strip for eight-band LTE/GSM/UMTS mobile phone, *IEEE Trans Antennas Propagat* 58 (2010), 3426–3431.
24. C.T. Lee and K.L. Wong, Planar monopole with a coupling feed and an inductive shorting strip for LTE/GSM/UMTS operation in the mobile phone, *IEEE Trans Antennas Propagat* 58 (2010), 2479–2483.
25. Y.W. Chi and K.L. Wong, Quarter-wavelength printed loop antenna with an internal printed matching circuit for GSM/DCS/PCS/UMTS operation in the mobile phone, *IEEE Trans Antennas Propagat* 57 (2009), 2541–2547.
26. C.H. Chang and K.L. Wong, Printed $\lambda/8$ -PIFA for penta-band WWAN operation in the mobile phone, *IEEE Trans Antennas Propagat* 57 (2009), 1373–1381.

© 2012 Wiley Periodicals, Inc.

DESIGN AND FABRICATION OF NOVEL MICROLENS–MICROMIRRORS ARRAY FOR INFRARED FOCAL PLANE ARRAY

Yan Jian-Hua, Ou Wen, Ou Yi, and Zhao Li-Jun

Institute of Microelectronics of Chinese Academy of Science, No. 3 Beitucheng, Beijing 100029, China; Corresponding author: terryyan0@gmail.com

Received 7 June 2011

ABSTRACT: A simple method on fabricating a novel structure of microlens–micromirrors array (MMA) with 100% fill factor and smooth surface profile is presented. The MMA has a special structure, which has a microlens array with foot diameter of 35 μm on the upper layer and a micromirrors array with top width of 50 μm and bottom width of 30 μm on the lower layer. These two arrays are connected by a thin layer of silicon. The new structure has potential to integrate with infrared focal plane arrays (IRFPAs). An analytical optical model is established and experimentally verified; results show that all of the incident infrared lights within a certain range can be absorbed by the photosensitive surface of IRFPAs with this structure. © 2012 Wiley Periodicals, Inc. *Microw Opt Technol Lett* 54:879–884, 2012; View this article online at wileyonlinelibrary.com. DOI 10.1002/mop.26722

Key words: microlens array; infrared focal plane array; micromirrors array; thermal reflow; KOH etching

1. INTRODUCTION

Microlens array plays a very important role in many applications, such as optical storage system, optical communication, and infrared imaging [1]. So far, various microlens arrays such as hexagonal microlens array [2], circular microlens array [3], square microlens array [4, 5] were developed, which raised the incident lights efficiency. However, these arrays have low fill factors that cause the incident lights between every two adjacent microlens cannot be focused onto the photosensitive surface. Although some design concepts such as thin microlens mold with no gaps by hot embossing method [6], hexagonal microlens array with no gaps by etching the space between every two adjacent microlens, or sputtering silicon to cover the space [2, 7] were proposed for designing high fill factor microlens array, these methods increased the cost and were very difficult to realize. Besides, the property of microlens would be very bad for it is difficult to control the surface shape [1]. Consequently, how to develop an effective fabrication process for a microlens array with high fill factor and controllable shape as well as excellent surface properties is an important achievement for MOEMS [1].

In this article, we present a novel structure with a microlens array and a micromirrors array and disclose its detailed design concept flow. Experiments show that the structure has 100% fill factor and a smooth contour profile with effective optical properties.

Figure 1 shows the scheme view of the conceptual design of the novel structure. The housing structure shown in Figure 1(a) contains three parts of silicon oxide, reverse trapezoidal structure, and silicon substrate. The silicon oxide severed as a mask to form the reverse trapezoidal cavity by KOH anisotropic etching [8]. The cavity was full of polymer glass that had been fully exposed in the UV light. On the inner surface of the reverse trapezoidal cavity, there was a thin aluminum film served as a mirror's surface and a thin silicon oxide film served as a protection layer on the aluminum film. Based on the building structure as shown in Figure 1(a), a certain thickness layer of silicon was